iScience
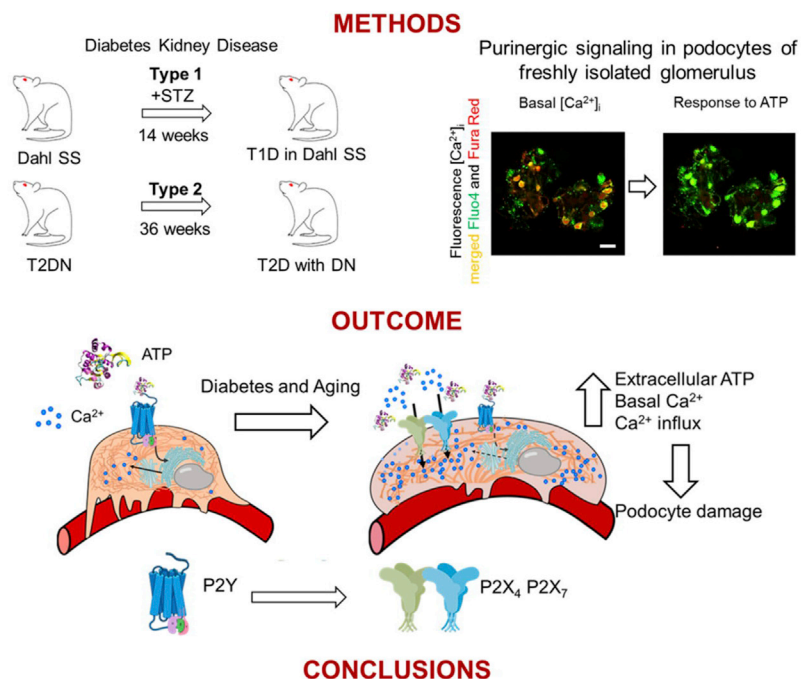
Article

Characterization of purinergic receptor 2 signaling in podocytes from diabetic kidneys

Remodeling of purinergic receptor 2 signaling in podocytes during the progression of diabetic kidney disease

METHODS

Diabetes Kidney Disease

Type 1
Dahl SS +STZ → T1D in Dahl SS
14 weeks

Type 2
T2DN 36 weeks → T2D with DN

Purinergic signaling in podocytes of freshly isolated glomerulus

Fluorescence [Ca²⁺]ᵢ merged Fluo4 and Fura Red

Basal [Ca²⁺]ᵢ   Response to ATP

OUTCOME

ATP
Ca²⁺   Diabetes and Aging →   ↑ Extracellular ATP
                                    Basal Ca²⁺
                                    Ca²⁺ influx
                                    ↓ Podocyte damage

P2Y → P2X₄ P2X₇

CONCLUSIONS

The pathological remodeling in purinergic signaling from metabotropic to ionotropic P2X₄ and P2X₇ receptors may contribute to podocyte loss and kidney injury in diabetes as it results in increased basal and ATP-stimulated [Ca²⁺]ᵢ likely exacerbating podocyte damage and apoptosis, and further aggravating DKD progression.

Oleg Palygin, Christine A. Klemens, Elena Isaeva, ..., Oksana Nikolaienko, Daria V. Ilatovskaya, Alexander Staruschenko

staruschenko@mcw.edu

Highlights

Diabetic podocytes have sustained intracellular Ca²⁺ signaling in response to ATP

Podocyte purinergic receptor signaling is predominantly ionotropic in diabetes

Both type 1 and 2 diabetic podocytes have similar purinergic receptor remodeling

Article

Characterization of purinergic receptor 2 signaling in podocytes from diabetic kidneys

Oleg Palygin,[1,2,5] Christine A. Klemens,[1,2,5] Elena Isaeva,[1,5] Vladislav Levchenko,[1] Denisha R. Spires,[1] Lashodya V. Dissanayake,[1] Oksana Nikolaienko,[1] Daria V. Ilatovskaya,[1,3] and Alexander Staruschenko[1,2,4,6,*]

SUMMARY

Growing evidence suggests that renal purinergic signaling undergoes significant remodeling during pathophysiological conditions such as diabetes. This study examined the renal P2 receptor profile and ATP-mediated calcium response from podocytes in glomeruli from kidneys with type 1 or type 2 diabetic kidney disease (DKD), using type 2 diabetic nephropathy (T2DN) rats and streptozotocin-injected Dahl salt-sensitive (type 1 diabetes) rats. A dramatic increase in the ATP-mediated intracellular calcium flux in podocytes was observed in both models. Pharmacological inhibition established that $P2X_4$ and $P2X_7$ are the major receptors contributing to the augmented ATP-mediated intracellular calcium signaling in diabetic podocytes. The transition in purinergic receptor composition from metabotropic to ionotropic may disrupt intracellular calcium homeostasis in podocytes resulting in their dysfunction and potentially further aggravating DKD progression.

INTRODUCTION

Diabetes is a severe chronic disorder characterized by impaired glucose metabolism mechanisms that leads to increased blood sugar levels, thereby damaging many vital corporeal systems, including cardiovascular, urinary, nervous systems, and vision. A major risk factor affecting patients with diabetes is an increased probability of developing diabetic kidney disease (DKD). Diabetes and its complications, including diabetic nephropathy (DN), are a significant cause of increased morbidity and mortality among people with diabetes, and a main risk factor for end-stage kidney disease. DN is a specific diagnosis referring to distinct pathologic structural and functional renal changes caused by diabetes and is distinguished by proteinuria, glomerular basement membrane thickening, mesangial expansion, GFR changes, and arterial hyalinosis, with progressive loss of renal function (Umanath and Lewis, 2018). Identification of mechanisms leading to DKD associated renal damage may accelerate the development of new therapies aiming to slow or prevent disease progression.

Clinical and experimental studies suggest that purinergic signaling is an important contributor to various physiological and pathophysiological processes in the kidney, including diabetes (Vallon et al., 2020). For example, ionotropic $P2X_7$ receptors are implicated in cyst formation in polycystic kidney disease and also renal interstitial inflammation associated with different kidney pathologies (Arkhipov et al., 2019; Chang et al., 2011; Goncalves et al., 2006; Taylor et al., 2009a). Renal proximal tubular $P2X_4$ activation promotes tubular inflammation and exacerbates ischemic acute kidney injury (Han et al., 2020), and deficient metabotropic $P2Y_2$ signaling has been shown to aggravate the progression of chronic kidney disease in mice (Potthoff et al., 2013). $P2Y_2$ was also reported as critical receptor in the control of ENaC-mediated sodium transport in the collecting duct (Mironova et al., 2019; Stockand et al., 2010). Furthermore, purinergic signaling is of additional interest due to the currently available pharmacopeia of P2 agonists and antagonists that may be useful therapeutic agents for various diseases, including hypertension and diabetes.

Microvascular dysfunction and alterations of glomerular filtration barrier (GFB) are early features of DKD progression. The GFB consists of endothelial cells, basement membrane, and podocytes (epithelial cells). Podocytes are highly specialized cells that maintain the integrity of the GFB, but progressive damage over time resulting from disease conditions causes podocyte loss and GFB dysfunction as they are non-proliferative. Diabetes can cause foot process effacement, podocyte cell death, and loss of GFB integrity, all of which are prognostic indicators of DKD (Mitrofanova et al., 2019; Vallon and Komers, 2011). We recently

[1]Department of Physiology, Medical College of Wisconsin, 8701 Watertown Plank Road, Milwaukee, WI 53226, USA

[2]Cardiovascular Center, Medical College of Wisconsin, Milwaukee, WI, USA

[3]Division of Nephrology, Department of Medicine, Medical University of South Carolina, Charleston, SC, USA

[4]Clement J. Zablocki Veterans Affairs Medical Center, Milwaukee, WI, USA

[5]These authors contributed equally

[6]Lead contact

*Correspondence: staruschenko@mcw.edu

https://doi.org/10.1016/j.isci.2021.102528

reported that in normal physiological conditions, $P2Y_1$ metabotropic signaling is the predominant mediator of intracellular Ca^{2+} ($[Ca^{2+}]_i$) flux in response to ATP in rat podocytes, where it helps regulate membrane potential and activity of transient receptor potential canonical (TRPC) channels (Ilatovskaya et al., 2013). Ionotropic P2X components may also be present in normal conditions, but their functional contribution is very low. In a streptozotocin (STZ) model of T1D, it was shown that $P2X_7$ receptors are absent in healthy controls, but become up-regulated in podocytes, endothelial, and mesangial cells (Vonend et al., 2004b). Also, human studies indicate $P2X_4$ and $P2X_7$ receptors are upregulated in T2D kidney tissue suggesting a role for these receptors in DN (Chen et al., 2013; Solini et al., 2013).

The aim of this study was to characterize podocyte purinergic signaling in type 1 diabetes (T1D) and type 2 diabetes (T2D) with DN. To do this, we used the type 2 diabetic nephropathy (T2DN) rat model whose renal phenotype has recently been thoroughly characterized (Nobrega et al., 2004; Palygin et al., 2019). T2DN rats were compared to non-diabetic control rats (Wistar) and diabetic rats that do not develop severe DN (Goto-Kakizaki [GK] (Goto et al., 1976)). For T1D, we utilized the established experimental model of streptozotocin (STZ)-injected Dahl salt-sensitive (SS) rats (Korner et al., 1997; Miller et al., 2018; Slaughter et al., 2013; Spires et al., 2018). We assessed the ATP-mediated $[Ca^{2+}]_i$ flux in podocytes during the progression of DKD. A distinct advantage of our approach is that podocyte signaling characterization is performed in podocytes of intact freshly isolated glomeruli; thus, the podocytes are exposed to whole organ and systemic changes until the end point experiments providing a more physiologically accurate environment than experiments conducted with cultured cells. The specific role of different subtypes of P2 receptors and the relative remodeling in $[Ca^{2+}]_i$ homeostasis were analyzed ex vivo using fluorescent confocal imaging of freshly isolated glomeruli and commercially available pharmacological tools. Our results demonstrate the purinergic receptor profile of podocytes in T1D and T2D have a significant increase in ionotropic calcium flux, mainly mediated by low affinity $P2X_4$ and $P2X_7$ receptors, whereas the contribution of metabotropic $P2Y_1$ signaling is decreased compared to healthy, non-diabetic podocytes. Furthermore, changes to basal Ca^{2+} concentrations and ATP response is present in early stage T2D diabetic kidneys before development of substantial renal damage. We verify that $P2X_4$ and $P2X_7$ activity is an additional pathological change which results in prolonged $[Ca^{2+}]_i$ levels and signaling, likely creating a feedforward mechanism that exacerbates podocyte apoptosis in the late-stages of diabetes. These results provide mechanistic insight into purinergic control of $[Ca^{2+}]_i$ in podocytes.

RESULTS

Experimental models of T1D and T2D

In order to characterize podocyte purinergic signaling in diabetes, we used well established models of T1D and T2D, namely the STZ-injected Dahl SS rat and the T2DN rat, respectively (Korner et al., 1997; Nobrega et al., 2004; Slaughter et al., 2013; Spires et al., 2018). Controls for T1D conditions were vehicle-injected Dahl SS rats, while for T2DN, controls included both a non-diabetic (Wistar) rat strain and a diabetic rat strain that does not develop severe DN (GK) rats (Palygin et al., 2019). The STZ-injected Dahl SS rat model closely mimics functional and morphological characteristics of human T1D DN, as it exhibits severe glomerulosclerosis, interstitial fibrosis, mesangial matrix expansion and proteinuria, and has previously been well characterized by us and others (Korner et al., 1997; Miller et al., 2018; Slaughter et al., 2013). Similarly, T2DN rats exhibit increased medullary protein casts, kidney fibrosis, and glomerular injury compared to GK or Wistar rats (Nobrega et al., 2004; Palygin et al., 2019). Diabetes and renal damage were verified by blood glucose levels and albuminuria (Figure 1). To assess changes in renal purinergic P2 signaling during early and late-stage T2D, male Wistar, GK, and T2DN rats at 12 and >48 weeks old were used. At the age of 12 weeks, both diabetic strains, T2DN and GK, display hyperglycemia but no significant albuminuria or change in total body weight (Figure 1B). At 48 weeks, T2DN rats show significant albuminuria, indicating glomerular disease. In our late-stage T1D model, blood glucose and albuminuria are substantially increased relative to controls, and total body weight is significantly decreased (Figure 1A).

Basal intracellular calcium levels and transient response to extracellular ATP is elevated in podocytes from T2D kidneys

To evaluate changes in intracellular calcium ($[Ca^{2+}]_i$) homeostasis and response to ATP in podocytes during T2D, we conducted live-cell Ca^{2+} fluorescence imaging in freshly isolated glomeruli from 12-week-old rats. Podocytes of T2DN rats have significantly greater basal $[Ca^{2+}]_i$ levels relative to non-diabetic (Wistar) or a diabetic rat without DN (GK), indicating cellular stress (Figure 2A). Acute application of ATP produced rapid transient activation of $[Ca^{2+}]_i$ in podocytes, as shown Figures 2B and 2C (see also Video S1). Activation of P2 receptors
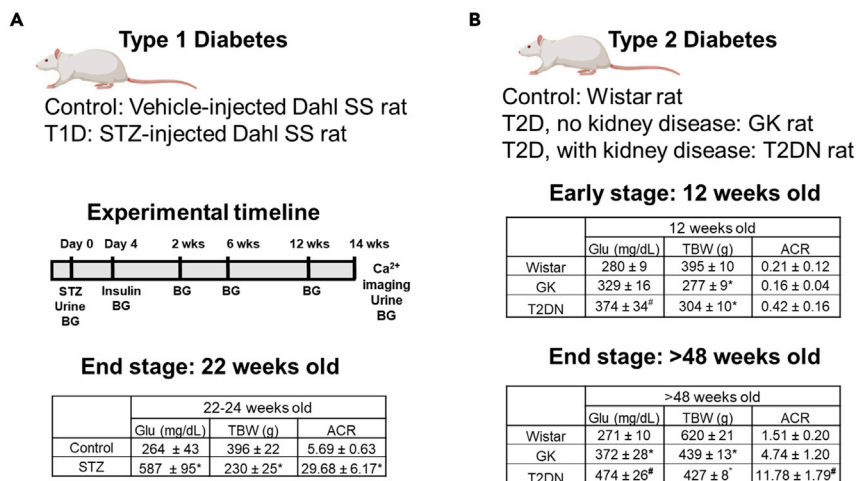
Figure 1. Experimental models of diabetes

(A) Experimental timeline for development of T1D. Rats were injected with streptozotocin (STZ) and had subcutaneous insulin pellets implanted 4 days later. Vehicle-injected control rats did not receive insulin. Blood glucose (BG) levels were tested periodically over the time course to verify consistently elevated glucose levels. After 14 weeks, terminal urine was collected and rats were sacrificed to collect tissue samples and isolate glomeruli for Ca^{2+} imaging. Terminal blood glucose (Glu), total body weight (TBW) and urinary albumin/creatinine ratios (ACR, $mg*dL^{-1}/mg*dL^{-1}$) are shown in the table. $N \geq 5$, values shown are mean $\pm$ SEM. Significance ($p < 0.05$) was determined by unpaired student t-test and is indicated by *.

(B) Characteristics of early (12 wks) and late stage (>48 wks) T2DN rats and controls. Glu, TBW, and ACR levels are shown in the inset tables. $N \geq 5$, values shown are mean $\pm$ SEM. Significance was determined by one-way ANOVA adjusted by Tukey's multiple-comparison. *$p < 0.05$ vs Wistar, #$p < 0.05$ vs. both Wistar and GK.

in T2DN rat podocytes is characterized by a prolonged $[Ca^{2+}]_i$ transient (Figure 2C), and significant increase in total $[Ca^{2+}]_i$ (calculated from area under the curve (AUC) from individual cell traces) The data are summarized in Figure 2D. These experiments demonstrate that podocytes have augmented basal and purinergic $[Ca^{2+}]_i$ signaling even before onset of clinically relevant renal damage indicators such as albuminuria.

Expression of P2 receptors in the renal cortex at different stages of DKD

In order to determine possible changes in purinergic signaling during the development of diabetic kidney injury in T2DN rats, we profiled P2 receptors expression in the renal cortex of 12- and 48-week-old animals. Figure 3 illustrates the expression of metabotropic $P2Y_1$, $P2Y_2$, and $P2Y_{12}$ (Figure 3A) and ionotropic $P2X_4$ and $P2X_7$ (Figure 3B) receptors in the cortical tissue of the 12-week-old Wistar, T2DN, and GK rats. The increase in the expression of $P2X_7$ protein was confirmed using a highly specific antibody directed against an extracellular epitope of $P2X_7$ (Figure 3B, bottom panel). Diabetic conditions at 12 weeks moderately affected the cortical abundance of metabotropic purinergic receptors with a significant decline in $P2Y_1$ expression in GK and trending decline in T2DN rats. In contrast, the expression of ionotropic $P2X_4$ and $P2X_7$ receptors was significantly elevated in both diabetic strains at 12 weeks of age (Figure 3B), similar what has been observed in patients with T2D (Chen et al., 2013; Solini et al., 2013). Interestingly, the expression of $P2X_4$ was more pronounced in aged T2DN than in GK rats, as the GK $P2X_4$ renal cortex expression was not significantly increased compared to Wistar in the aged (>48 weeks old) rats (Figure 4B). In 48-week-old rats, $P2Y_1$ was significantly decreased in both GK and T2DN rats (Figure 4). In addition, mRNA levels were assessed in the cortical renal tissue of 12-week-old animals using qPCR analysis. Our data show a dramatic change in *P2rx4* and *P2rx7* gene expression without alteration of *P2ry1* and *P2ry2* expression in the renal cortex of GK and T2DN rats compared to non-diabetic Wistar rats (Figure S1).

P2 receptor signaling in podocytes of DN rats

In our previous study, we demonstrated that $P2Y_1$ is the major purinoreceptor contributing to ATP-induced $[Ca^{2+}]_i$ response in rat podocytes under normal physiological conditions (Ilatovskaya et al., 2013). However, Western blot and qPCR data from kidney cortex of control and T2DN rats indicate that there is a substantial change in the expression profile of various P2 receptors in the renal cortex of diabetic rats with a shift of their balance from metabotropic to ionotropic signaling. To test the functional presence of $P2X_4$ and
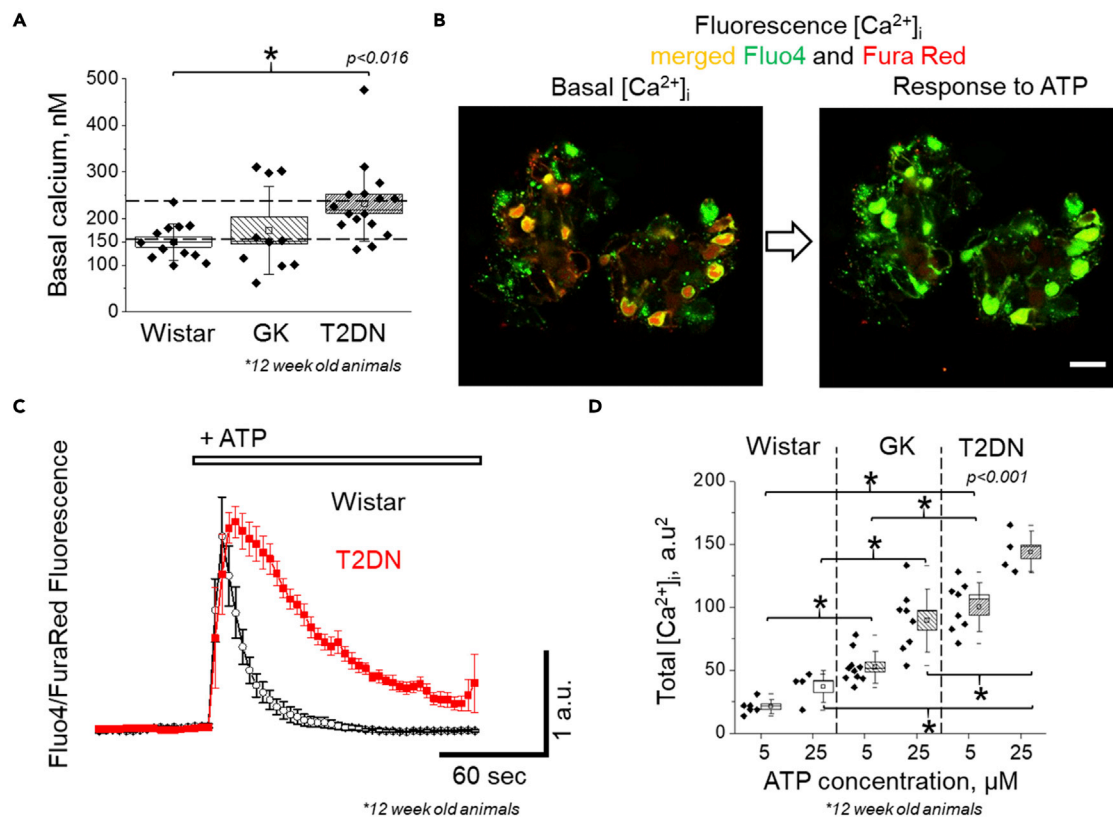
Figure 2. Changes in basal and ATP-mediated intracellular Ca²⁺ ([Ca²⁺]ᵢ) response in podocytes of freshly isolated glomeruli from control and type 2 diabetic rats

(A) Summary graph showing an increase in basal $[Ca^{2+}]_i$ in podocytes of T2DN compared to Wistar rats.

(B) Representative images of a glomerulus freshly isolated from 12-week-old T2DN rat and loaded with Fluo-4 (green pseudocolor) and Fura Red AM (red pseudocolor) calcium dyes made before and after application of ATP.

(C) Examples of the ATP-induced $[Ca^{2+}]_i$ transients simultaneously recorded from several podocytes in glomeruli isolated from age-matched Wistar (black) or T2DN (red) rats. Note the much slower decay of $[Ca^{2+}]_i$ transient is observed in podocytes of T2DN rats.

(D) Summary graph showing a $[Ca^{2+}]_i$ increase in response to 5 and 25 μM ATP application in podocytes of 12 weeks old Wistar, GK and T2DN rats. ANOVA test significance ($p < 0.05$) is indicated by *, Tukey's multiple-comparison adjustment was applied. In the box plot graphs, the box represents ± SE, and a line inside the box marks the median. The whiskers are ± SD.

P2X₇ receptors in podocytes during advanced DN, we investigated the effect of pharmacological inhibition of ATP-mediated $[Ca^{2+}]_i$ flux in adult T2DN rats (>48-weeks-old). Application of ATP produces a robust transient response in podocytes from freshly isolated T2DN glomeruli (Figure 5, representative transients without inhibitors are in gray). The ATP-induced $[Ca^{2+}]_i$ response was significantly blunted in the presence of specific P2X₄ (10 μM 5-BDBD) or P2X₇ (10μM A 438079) antagonists and was dramatically reduced when both P2X₄ and P2X₇ antagonists were combined, indicating a major contribution of these receptors to ATP-mediated $[Ca^{2+}]_i$ signaling in podocytes of T2DN rats (Figure 5).

Characterization of renal P2 receptors in T1D

Figure 6A (see also Video S2) shows representative images of $[Ca^{2+}]_i$ fluorescence changes in podocytes of freshly isolated glomeruli from control and T1D rats before (baseline image), at peak response, and 5 min post ATP application. The ATP-induced $[Ca^{2+}]_i$ transient in podocytes from T1D rats has a significantly reduced peak amplitude compared to controls and larger $[Ca^{2+}]_i$ transient (Figures 6B–6D). These results demonstrate temporal differences in $[Ca^{2+}]_i$ signaling, suggesting likely augmentation in P2-mediated calcium entry and changes in the podocyte purinergic receptor expression profile in T1D. Importantly, the signal is prolonged and does not return to baseline within the time period measured suggesting disruption of homeostatic Ca²⁺ signaling pathways.
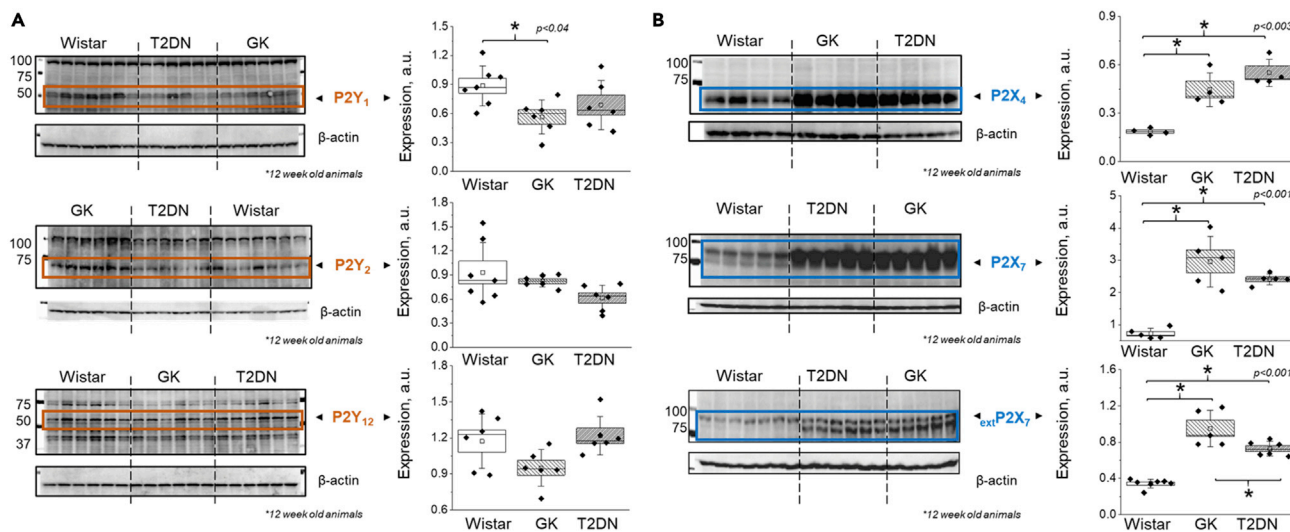
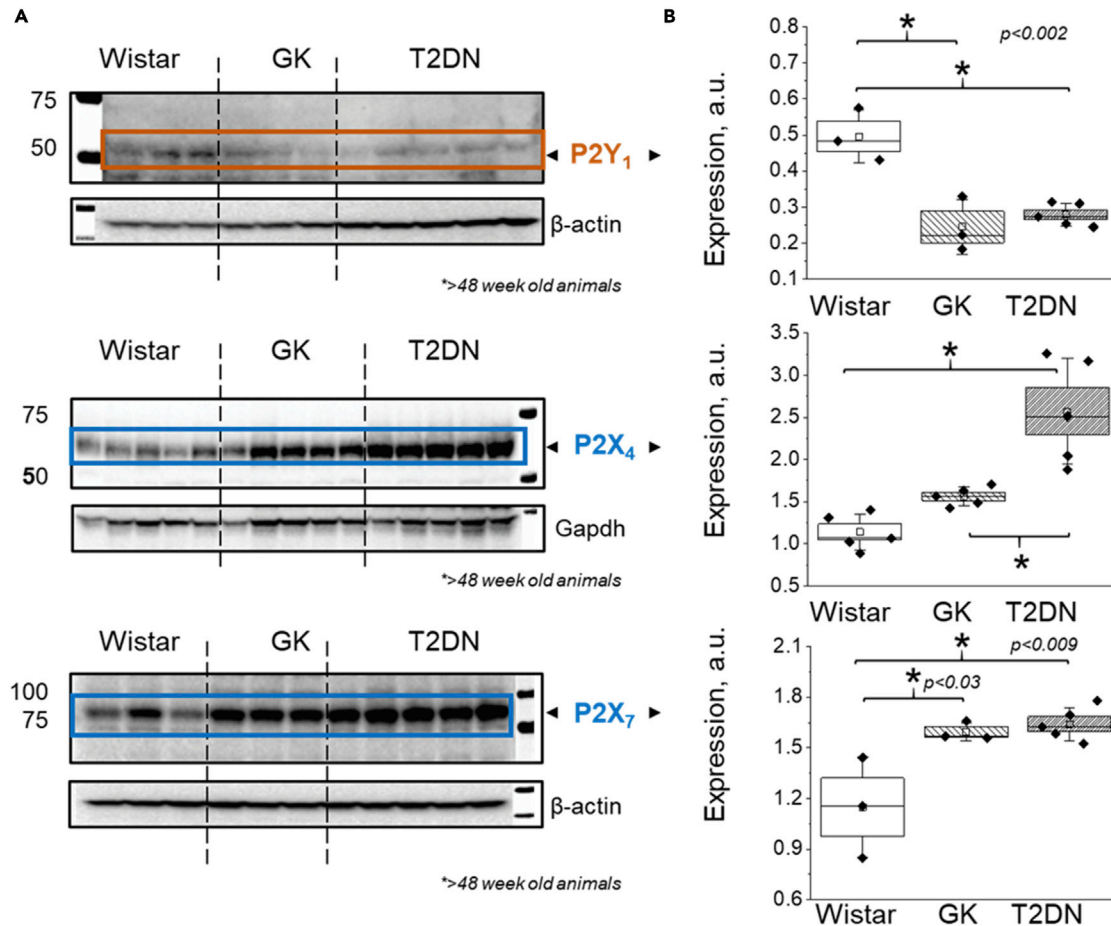**Figure 3. Expression of P2 receptors in renal cortex of young rats**

(A) Western blot images and corresponding summary graphs showing densitometry of metabotropic (depicted in brown) $P2Y_1$, $P2Y_2$ and $P2Y_{12}$ protein expression levels in renal cortex of 12-weeks-old Wistar, GK and T2DN rats.

(B) Western blot images and corresponding summary graphs showing densitometric analysis of ionotropic (depicted in blue) $P2X_4$ and $P2X_7$ protein expression levels in renal cortex of 12-weeks-old Wistar, GK and T2DN rats. All Western blot values were normalized to loading control (β-actin). Significance (p < 0.05) is indicated by *, Tukey's multiple-comparison adjustment was applied. In the box plot graphs, the box represents ± SE, and a line inside the box marks the median. The whiskers are ± SD.

To delineate the contribution of various P2 receptors in ATP-induced $[Ca^{2+}]_i$ signaling in T1D podocytes, specific blockers of metabotropic $P2Y_1$ (MRS2500) and ionotropic $P2X_4$ and $P2X_7$ receptors (5-BDBD; A438079) were used. Summary transients recorded from T1D podocytes pretreated with inhibitor (black) compared to untreated T1D podocytes (gray) and control podocytes (light gray) are shown in Figure 7A. Using AUC measurements to determine the magnitude of $[Ca^{2+}]_i$ over the time period, and calculating them as a percentage of the AUC measurement from untreated T1D podocytes allowed us to determine the percent contribution of the different P2 receptors. This percentage of inhibition is shown in Figure 7B and summarizes the effect of application of $P2Y_1$, $P2X_4$ and $P2X_7$ either alone or in combination on $[Ca^{2+}]_i$ response. Treatment with the $P2Y_1$ antagonist had a moderate effect on the $[Ca^{2+}]_i$ transient (~15% reduction). Inhibition of $P2X_4$ or $P2X_7$ reduced the prolonged $[Ca^{2+}]_i$ signal (~40% and ~26%, correspondingly). Antagonism of both $P2X_4$ and $P2X_7$ resulted in a response curve more closely resembling the transient signal of healthy podocytes, and these ionotropic receptors contributed to ~43% block of the calcium signal. Finally, pretreatment of T1D glomeruli with all three inhibitors substantially decreased podocyte $[Ca^{2+}]_i$ response to 40 μM ATP, suggesting $P2Y_1$, $P2X_4$, and $P2X_7$ account for ~80% of the total $[Ca^{2+}]_i$ transient. These data indicate that, in contrast to data obtained previously from podocytes of healthy Sprague-Dawley rats (Ilatovskaya et al., 2013), both T1D and T2D conditions result in a dramatic shift to ionotropic P2 receptor ATP-induced Ca^{2+} flux. We also verified that pretreatment with $P2X_4$ and $P2X_7$ inhibitors does not affect the ATP-evoked $[Ca^{2+}]_i$ transient in healthy, age-matched control Dahl SS rats (Figure S2), demonstrating that similar to our previous results in Sprague-Dawley rats, functionally active $P2X_4$ or $P2X_7$ are not a major contributor to healthy Dahl SS podocyte ATP-mediated $[Ca^{2+}]_i$ response. The presence of $P2X_4$ in diabetic podocytes was also verified by immunofluorescent labeling of $P2X_4$ with the podocyte-marker, nephrin, in a freshly isolated T1D glomerulus (Figure S3).

DISCUSSION

Under normal physiological conditions, extracellular ATP levels are low due to the activity of numerous ATP-metabolizing endogenous enzymes (Schwiebert and Zsembery, 2003); however pathological changes result in increased extracellular ATP concentrations and purinergic signaling. We previously demonstrated that basal extracellular concentrations of ATP in the renal cortex can go as high as 400 nM (Palygin et al., 2013), that extracellular ATP increases dramatically in response to increased renal perfusion pressure

Figure 4. Expression of P2 receptors in renal cortex of old rats

Western blot images and corresponding summary graphs showing densitometric analysis of P2Y$_1$ (A), P2X$_4$ and P2X$_7$ (B) protein expression levels in renal cortex of the aged (>48-weeks-old) Wistar, GK and T2DN rats. All Western blot values were normalized to loading control (β-actin or Gapdh). Significance (p < 0.05) is indicated by *, Tukey's multiple-comparison adjustment was applied. In the box plot graphs, the box represents $\pm$ SE, and a line inside the box marks the median. The whiskers are $\pm$ SD.

(Palygin et al., 2017), and that in pathological conditions like PKD, ATP levels can exceed 1μM (Palygin et al., 2018). In agreement with these findings, human studies have found significant increases in the plasma levels of purine metabolites of patients with DN compared to patients with T2D without nephropathy (Xia et al., 2009). Pathological changes resulting from diabetes, especially in the late stages with multi-organ systemic damage, may potentially increase extracellular ATP concentrations in the kidney, therefore greater insight into the purinergic signaling profile of diabetic podocytes is essential to further therapeutic treatment options (Burnstock and Novak, 2013).

Functionally, all three diabetic rats (GK, T2DN, and STZ-induced T1D) demonstrated augmented ATP-mediated [Ca^{2+}]$_i$ responses compared to age-matched non-diabetic Wistar and Dahl SS rats. This alternation in Ca^{2+} homeostasis could lead to a number of detrimental cellular processes, including cytoskeletal modifications that alter cell shape and foot process dynamics; activation of Ca^{2+}-dependent catabolic enzymes (proteases, phospholipases, endonucleases) causing membrane damage, and signaling pathways leading to cell death. The deleterious nature of excessive intracellular Ca^{2+} and its association with apoptosis has been well established for several decades (Fleckenstein et al., 1983; Nicotera and Orrenius, 1998; Rizzuto et al., 2003). Calcium overload can occur through both intra- and extracellular routes, and dysregulation of these homeostatic mechanisms has been shown to be associated with cell death in a number of different cell types (Fleckenstein et al., 1983; Nicotera and Orrenius, 1998; Rizzuto et al., 2003). While we have not directly confirmed that the increased basal Ca^{2+} and
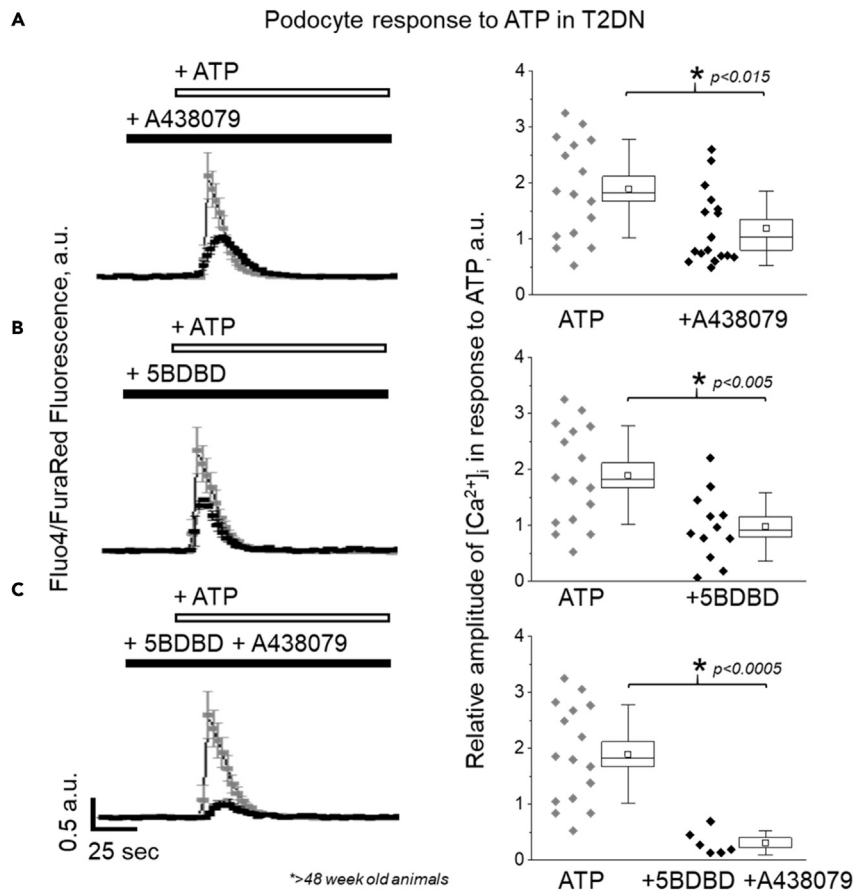
Figure 5. Ionotropic P2X$_4$ and P2X$_7$ receptors play a predominant role in ATP-induced increase in [Ca^{2+}]$_i$ in podocytes of T2DN rats

Summary of changes in the ATP evoked [Ca^{2+}]$_i$ transient in the absence or presence of P2X$_4$ and P2X$_7$ antagonists separately or together: (A) 10 μM A438079 - P2X$_7$ antagonist; (B) 10 μM 5-BDBD - P2X$_4$ inhibitor, and (C) both antagonists in T2DN rats. [Ca^{2+}]$_i$ transients were induced by application of 100 μM ATP.

Summary graphs to the right of the averaged response show the relative amplitude of ATP-induced [Ca^{2+}]$_i$ flux. * indicates statistical significance (p < 0.05) as determined by student t-test. In the box plot graphs, the box represents $\pm$ SE, and a line inside the box marks the median. The whiskers are $\pm$ SD.

augmented Ca^{2+} transients lead to apoptosis in our diabetic podocytes, future studies will more thoroughly verify this transition from this excess [Ca^{2+}]$_i$ to apoptosis or other forms of cell death by assessing caspase cleavage and DNA breakage in podocytes from isolated glomeruli following acute ATP application or inactive ATP analog.

Under normal physiological conditions in podocytes, metabotropic G protein-coupled receptor signaling (including P2Y$_1$, P2Y$_2$ and P2Y$_6$) predominates and works by activating TRPC6 signaling and regulating ROS production in the cell (Burford et al., 2014; Fischer et al., 2001; Roshanravan and Dryer, 2014). Our studies demonstrate diabetic podocytes have a distinct purinergic signaling profile compared to non-diabetic podocytes with augmented ATP-mediated [Ca^{2+}]$_i$ flux; however, what specific trigger or combination of stimuli in diabetes causes this transition remains to be determined. Potential causes may include increased blood glucose concentrations, immune cell infiltration, altered blood pressure, glomerular perfusion pressure, altered extracellular ATP levels or a range of factors, and additional experiments, such as those that would allow for continuous glucose control in rats by preventing or inducing hyperglycemia will more methodically delineate these potential causes.
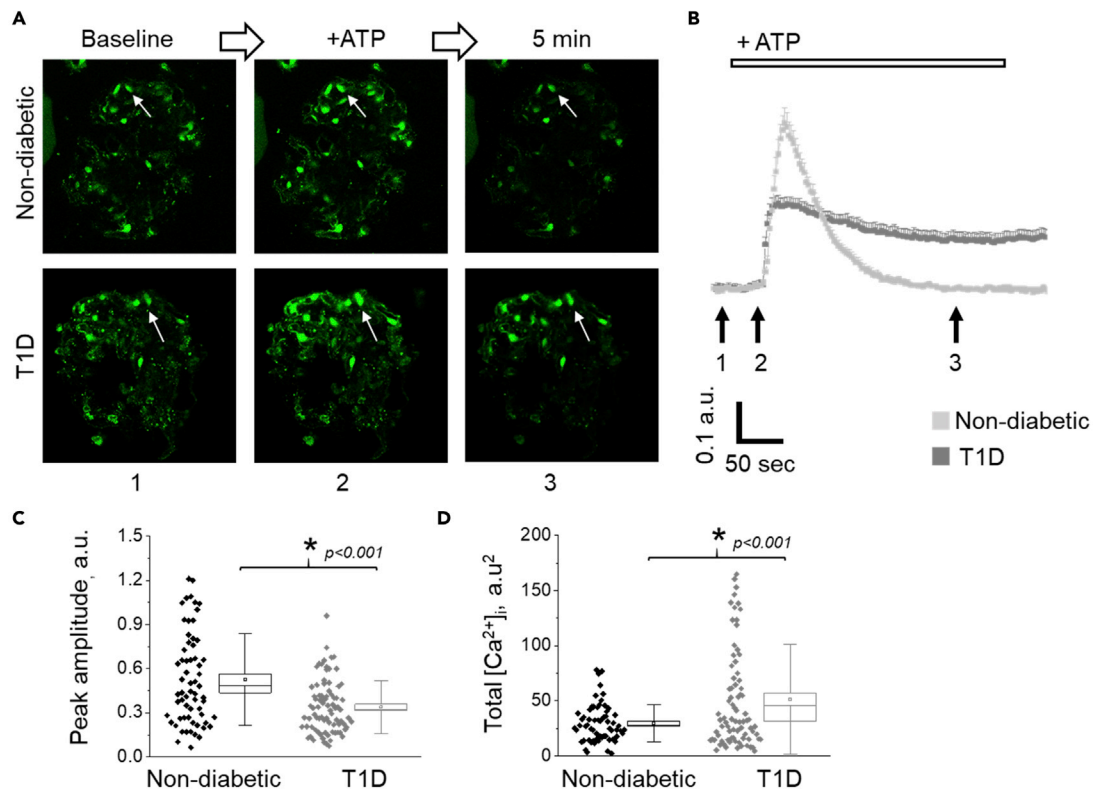
Figure 6. Intracellular Ca²⁺ [Ca²⁺]ᵢ response to ATP in T1D

(A) Representative images of control or T1D glomeruli at baseline (1), immediately following application of 40 μM ATP (2), or 5 min post application (3). Glomeruli were isolated from STZ- (T1D) or vehicle-injected control Dahl SS rats loaded with Fluo4 and FuraRed dyes for ratiometric calcium imaging. Note the prolonged signal in the T1D podocytes compared to controls (arrows). Only images from the Fluo4 channel are shown.

(B) Averaged curves of [Ca²⁺]ᵢ changes from control (light gray) or T1D (gray) podocytes. Arrows indicate time points (1, 2, and 3) of images shown in (A). Summarized data of the (C) peak amplitude and (D) [Ca²⁺]ᵢ transient (quantified as the total area under the curve) in response to ATP in STZ-SS and control rats. Individual points are cells. * indicates statistical significance, p < 0.05, as determined by unpaired student t-test. In the box plot graphs, the box represents ± SE, and a line inside the box marks the median. The whiskers are ± SD.

Our experiments in both T1D and T2D podocytes with specific inhibitors provide compelling evidence that P2X₄ and P2X₇ receptors play a major role in ATP-induced [Ca²⁺]ᵢ levels in diabetic podocytes. Previous research has established that P2X₇ receptor expression increases are linked to PKD, glomerulonephritis, human lupus nephritis, and hypertension-associated renal injury (Arkhipov et al., 2019; Hillman et al., 2005; Pereira et al., 2020; Vallon et al., 2020). In addition, the upregulation of glomerular P2X₇ receptor mRNA and protein expression has been reported in STZ-induced diabetic and ren-2 transgenic hypertensive rat models, and was associated with inflammatory cytokine release and cell death (Vonend et al., 2004a). Studies have also shown that pharmacological inhibition or deletion of P2X₇ receptor offers varying degrees of protection in these pathologies (Arkhipov et al., 2019; Ji et al., 2012; Menzies et al., 2015, 2017a, 2017b; Pereira et al., 2020; Taylor et al., 2009b). Here we show that podocytes in late-stage diabetes mellitus have direct ionotropic P2 calcium entry through the pore-forming P2X₄, and P2X₇ channels in addition to metabotropic signaling through P2Y₁. While still speculative, this ATP-mediated Ca²⁺ flux in podocytes may contribute to pathological changes in diabetes by instigating cell damage and podocyte cell death. Our data also demonstrate significant differences in renal cortex expression of several P2 receptors in diabetes; however, it is important to note that these changes occur in whole kidney cortex lysates, and direct comparisons to the functional podocyte signaling data cannot be made.

Although we did not interrogate functional P2 activity for all glomerular cells in diabetes in the present work, a few recent single-cell transcriptomic studies have begun to investigate transcriptomic profiles in individual cells (Chung et al., 2020; Fu et al., 2019; Wilson et al., 2019). Of particular interest is the study from Wilson et al. (2019) profiling single-cell transcriptomics from early human DN, and the easily
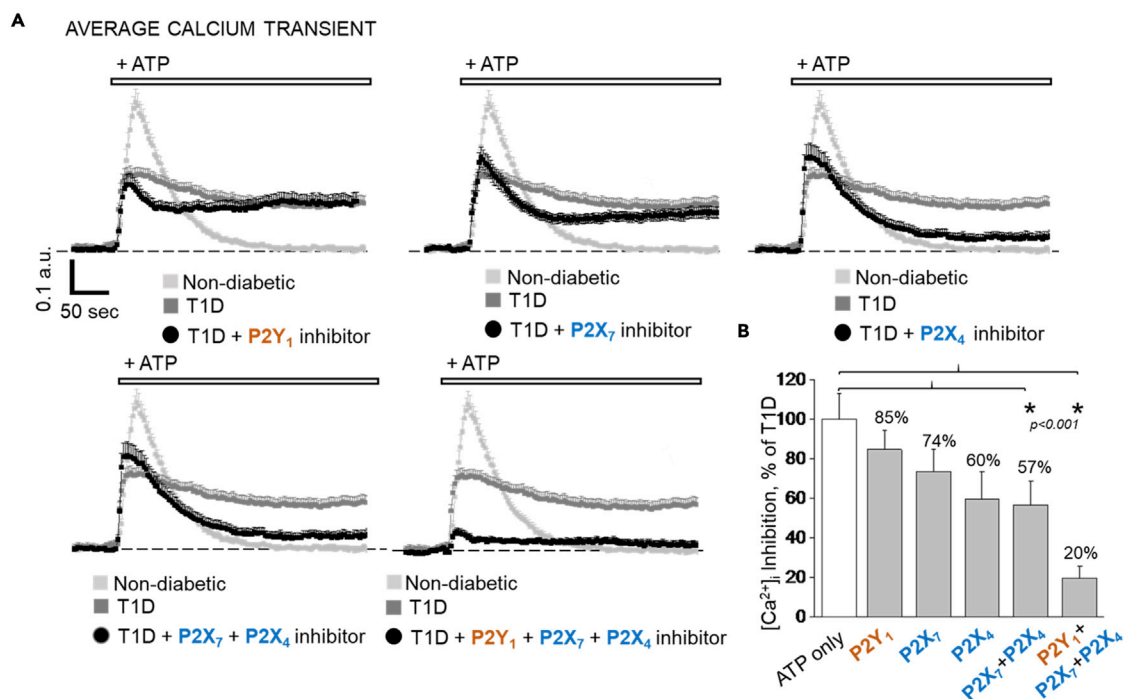
Figure 7. Effects of P2 receptor inhibition on [Ca²⁺]ᵢ handling in T1D

(A) Summarized ATP (40 μM) response curves from podocytes in the presences of a P2 antagonist (black) versus T1D (gray, no inhibitor) or non-diabetic (light gray). Shown are effects of pre-incubation with 1 μM MRS2500 (P2Y₁ antagonist), 10 μM A438079 (P2X₇ antagonist), 10 μM 5-BDBD (P2X₄ inhibitor), both P2X receptor antagonists, and with antagonists targeting all 3 P2 receptors.

(B) Summarized [Ca²⁺]ᵢ transient as a percentage of T1D [Ca²⁺]ᵢ response in the presence of P2Y₁, P2X₄ and P2X₇ antagonists from curves shown in (A). Significance (p < 0.05) is indicated by *, One-way ANOVA with Dunnett's multiple-comparison adjustment was applied. Values shown in B are mean ± SEM.

searchable online data set provided by the Humphrey Lab available at http://humphreyslab.com/SingleCell/(Wilson et al., 2019). Using the search function of the human diabetic kidney set, podocyte-specific changes in P2 receptor expression can be easily queried by gene name. Similar to our functional results, in this dataset *P2RX7* expression increases while *P2RY1* expression decreases. There appears to be no change in *P2RY2* or *P2RX4* expression. The advantage of our study is that it shows the profound functional affects resulting from this unique purinergic profile, namely different calcium signaling responses to ATP and potential dysregulation of basal calcium homeostasis. This provides greater mechanistic support to the idea that the increased contribution of P2X₄ and P2X₇ receptor activity to ATP-dependent Ca²⁺ dynamics occurring in diabetes may exacerbate DN damage in podocytes. Also of note is the potential for P2X₄ and P2X₇ to interact and influence the electrophysiological properties of one another, although this interaction is still under debate (Craigie et al., 2013; Guo et al., 2007; Nicke, 2008; Perez-Flores et al., 2015; Schneider et al., 2017). P2X₄ and P2X₇ are able to co-immunoprecipitate with one another (Guo et al., 2007), and some studies have shown functional current changes when P2X₄ and P2X₇ are co-expressed suggesting they form heteromers (Guo et al., 2007), although others have not (Nicke, 2008). While only conjecture, altered current kinetics resulting from P2X₄/P2X₇ heteromers may explain the prolonged calcium signal observed in the late stage T1D podocytes which fails to return to baseline levels. Additionally, while P2X₄ is present in both normal and diabetic podocytes, perhaps it requires the upregulation of P2X₇ that occurs in late-stage diabetes in order to influence ATP-mediated [Ca²⁺]ᵢ. Further studies are needed to examine this potential interaction in diabetic podocytes.

In summary, these data demonstrate the dramatic increase in ionotropic P2 receptor podocyte signaling, with P2X₄ and P2X₇ contributing to ATP-mediated [Ca²⁺]ᵢ flux in DKD in both T1D and T2D. Future studies treating T1D or T2D rats during the development of end stage diabetes with P2X₄ and P2X₇ antagonists will determine whether pharmacological intervention may be able to attenuate pathological Ca²⁺ signaling and prevent exacerbation of cellular damage and apoptosis.

Limitations of the study

While we feel the data from these experiments provides strong support for the change in ATP-mediated signaling from metabotropic to ionotropic signaling in diabetic podocytes, this study still has several limitations. First, this study utilized males and did not examine potential sexual dimorphisms in purinergic podocyte signaling, which will be interesting to examine in future studies. Additionally, this study did not take into consideration potential differences from diet. Dahl SS rats (vehicle- and STZ-injected) were maintained on standard 0.4% NaCl AIN-76 diet (#D113755), whereas the Wistar/GK/T2DN rats were maintained on a Purina LabDiet (Cat#5001). Transcriptional and translational changes in purinergic receptor expression profiles were determined from kidney cortex rather than glomerular fractions due to the limited availability of *ex vivo* tissue for experiments; therefore the reported expression changes are global rather than podocyte-specific, so comparisons of the Western blot results to direct functional data of podocyte signaling cannot be made without further co-localization studies. Experimentally, one technical flaw is the inability to pressurize our glomeruli. Structural components are essential to podocyte function and it is possible that lack of oncotic or hydrostatic pressure, flow, or membrane stretch may impact purinergic response. This is particularly of note as $P2X_4$ has been proposed to function as a mechanosensory protein in podocytes to modify cytoskeletal organization, and lack of mechanical perturbation may be the reason we do no observe $P2X_4$ activity in healthy podocytes (Forst et al., 2016). Lastly, while it is likely that excessive Ca^{2+} signaling from ionotropic P2 receptors in diabetic podocytes exacerbates podocyte damage, whether this remodeling is causative and occurs in early stages of the disease in podocytes or is a response to early pathological changes is still up for debate. Repeating these experiments with conditional or cell-specific knockouts or in glucose-controlled diabetic animals in future experiments could help uncover this chicken or egg dilemma.

STAR★METHODS

Detailed methods are provided in the online version of this paper and include the following:

- KEY RESOURCES TABLE
- RESOURCE AVAILABILITY
  - Lead contact
  - Materials availability
  - Data and code availability
- EXPERIMENTAL MODEL AND SUBJECT DETAILS
  - Animals
- METHOD DETAILS
  - Glomeruli isolation
  - Confocal calcium imaging in the podocytes of freshly isolated glomeruli
  - Western blotting
  - mRNA isolation and PCR analysis
  - Immunofluorescence labeling
- QUANTIFICATION AND STATISTICAL ANALYSIS

SUPPLEMENTAL INFORMATION

Supplemental information can be found online at https://doi.org/10.1016/j.isci.2021.102528.

AUTHOR CONTRIBUTIONS

OP, CAK, EI, DVI, and AS designed the study; OP, CAK, EI, VVL, DS, LVD, and DVI performed the investigations; DVI, OP, CAK, LVD, ON, and EI analyzed the data; OP, CAK, EI, and DVI made the figures; OP, CAK, EI, DVI, and AS drafted and revised the paper. All authors approved the final version of the manuscript.

DECLARATION OF INTERESTS

The authors declare no competing interests.

REFERENCES

Arkhipov, S.N., Potter, D.L., Geurts, A.M., and Pavlov, T.S. (2019). Knockout of P2rx7 purinergic receptor attenuates cyst growth in a rat model of ARPKD. Am. J. Physiol. Ren. Physiol. 317, F1649–F1655.

Burford, J.L., Villanueva, K., Lam, L., Riquier-Brison, A., Hackl, M.J., Pippin, J., Shankland, S.J., and Peti-Peterdi, J. (2014). Intravital imaging of podocyte calcium in glomerular injury and disease. J. Clin. Invest. 124, 2050–2058.

Burnstock, G., and Novak, I. (2013). Purinergic signalling and diabetes. Purinergic Signal. 9, 307–324.

Chang, M.Y., Lu, J.K., Tian, Y.C., Chen, Y.C., Hung, C.C., Huang, Y.H., Chen, Y.H., Wu, M.S., Yang, C.W., and Cheng, Y.C. (2011). Inhibition of the P2X7 receptor reduces cystogenesis in PKD. J. Am. Soc. Nephrol. 22, 1696–1706.

Chen, K., Zhang, J., Zhang, W., Zhang, J., Yang, J., Li, K., and He, Y. (2013). ATP-P2X4 signaling mediates NLRP3 inflammasome activation: a novel pathway of diabetic nephropathy. Int. J. Biochem. Cell Biol. 45, 932–943.

Chung, J.J., Goldstein, L., Chen, Y.J., Lee, J., Webster, J.D., Roose-Girma, M., Paudyal, S.C., Modrusan, Z., Dey, A., and Shaw, A.S. (2020). Single-cell transcriptome profiling of the kidney glomerulus identifies Key cell types and reactions to injury. J. Am. Soc. Nephrol. 31, 2341–2354.

Craigie, E., Birch, R.E., Unwin, R.J., and Wildman, S.S. (2013). The relationship between P2X4 and P2X7: a physiologically important interaction? Front. Physiol. 4, 216.

Fischer, K.G., Saueressig, U., Jacobshagen, C., Wichelmann, A., and Pavenstadt, H. (2001). Extracellular nucleotides regulate cellular functions of podocytes in culture. Am. J. Physiol. Ren. Physiol. 281, F1075–F1081.

Fleckenstein, A., Frey, M., and Fleckenstein-Grun, G. (1983). Consequences of uncontrolled calcium entry and its prevention with calcium antagonists. Eur. Heart J. 4, 43–50.

Forst, A.L., Olteanu, V.S., Mollet, G., Wlodkowski, T., Schaefer, F., Dietrich, A., Reiser, J., Gudermann, T., Mederos y Schnitzler, M., and Storch, U. (2016). Podocyte purinergic P2X4 channels are mechanotransducers that mediate cytoskeletal disorganization. J. Am. Soc. Nephrol. 27, 848–862.

Fu, J., Akat, K.M., Sun, Z., Zhang, W., Schlondorff, D., Liu, Z., Tuschl, T., Lee, K., and He, J.C. (2019). Single-cell RNA profiling of glomerular cells shows dynamic changes in experimental diabetic kidney disease. J. Am. Soc. Nephrol. 30, 533–545.

Goncalves, R.G., Gabrich, L., Rosario, A., Jr., Takiya, C.M., Ferreira, M.L., Chiarini, L.B., Persechini, P.M., Coutinho-Silva, R., and Leite, M., Jr. (2006). The role of purinergic P2X7 receptors in the inflammation and fibrosis of unilateral ureteral obstruction in mice. Kidney Int. 70, 1599–1606.

Goto, Y., Kakizaki, M., and Masaki, N. (1976). Production of spontaneous diabetic rats by repetition of selective breeding. Tohoku J. Exp. Med. 119, 85–90.

Guo, C., Masin, M., Qureshi, O.S., and Murrell-Lagnado, R.D. (2007). Evidence for functional P2X4/P2X7 heteromeric receptors. Mol. Pharmacol. 72, 1447–1456.

Han, S.J., Lovaszi, M., Kim, M., D'Agati, V., Hasko, G., and Lee, H.T. (2020). P2X4 receptor exacerbates ischemic AKI and induces renal proximal tubular NLRP3 inflammasome signaling. FASEB J. 34, 5465–5482.

Hillman, K.A., Burnstock, G., and Unwin, R.J. (2005). The P2X7 ATP receptor in the kidney: a matter of life or death? Nephron Exp. Nephrol. 101, e24–30.

Ilatovskaya, D.V., Blass, G., Palygin, O., Levchenko, V., Pavlov, T.S., Grzybowski, M.N., Winsor, K., Shuyskiy, L.S., Geurts, A.M., Cowley, A.W., Jr., et al. (2018). A NOX4/TRPC6 pathway in podocyte calcium regulation and renal damage in diabetic kidney disease. J. Am. Soc. Nephrol. 29, 1917–1927.

Ilatovskaya, D.V., Levchenko, V., Lowing, A., Shuyskiy, L.S., Palygin, O., and Staruschenko, A. (2015). Podocyte injury in diabetic nephropathy: implications of angiotensin II-dependent activation of TRPC channels. Sci. Rep. 5, 17637.

Ilatovskaya, D.V., Palygin, O., Levchenko, V., and Staruschenko, A. (2013). Pharmacological characterization of the P2 receptors profile in the podocytes of the freshly isolated rat glomeruli. Am. J. Physiol. Cell Physiol. 305, C1050–C1059.

Ji, X., Naito, Y., Weng, H., Endo, K., Ma, X., and Iwai, N. (2012). P2X7 deficiency attenuates hypertension and renal injury in deoxycorticosterone acetate-salt hypertension. Am. J. Physiol. Ren. Physiol. 303, F1207–F1215.

Korner, A., Jaremko, G., Eklof, A.C., and Aperia, A. (1997). Rapid development of glomerulosclerosis in diabetic Dahl salt-sensitive rats. Diabetologia 40, 367–373.

Menzies, R.I., Booth, J.W.R., Mullins, J.J., Bailey, M.A., Tam, F.W.K., Norman, J.T., and Unwin, R.J. (2017a). Hyperglycemia-induced renal P2X7 receptor activation enhances diabetes-related injury. EBioMedicine 19, 73–83.

Menzies, R.I., Howarth, A.R., Unwin, R.J., Tam, F.W., Mullins, J.J., and Bailey, M.A. (2015). Inhibition of the purinergic P2X7 receptor improves renal perfusion in angiotensin-II-infused rats. Kidney Int. 88, 1079–1087.

Menzies, R.I., Tam, F.W., Unwin, R.J., and Bailey, M.A. (2017b). Purinergic signaling in kidney disease. Kidney Int. 91, 315–323.

Miller, B.S., Blumenthal, S.R., Shalygin, A., Wright, K.D., Staruschenko, A., Imig, J.D., and Sorokin, A. (2018). Inactivation of p66Shc decreases afferent arteriolar KATP channel activity and decreases renal damage in diabetic Dahl SS rats. Diabetes 67, 2206–2212.

Mironova, E., Suliman, F., and Stockand, J.D. (2019). Renal Na(+) excretion consequent to pharmacogenetic activation of G(q)-DREADD in principal cells. Am. J. Physiol. Ren. Physiol. 316, F758–f767.

Mitrofanova, A., Sosa, M.A., and Fornoni, A. (2019). Lipid mediators of insulin signaling in diabetic kidney disease. Am. J. Physiol. Ren. Physiol. 317, F1241–f1252.

Nicke, A. (2008). Homotrimeric complexes are the dominant assembly state of native P2X7 subunits. Biochem. Biophys. Res. Commun. 377, 803–808.

Nicotera, P., and Orrenius, S. (1998). The role of calcium in apoptosis. Cell Calcium 23, 173–180.

Nobrega, M.A., Fleming, S., Roman, R.J., Shiozawa, M., Schlick, N., Lazar, J., and Jacob, H.J. (2004). Initial characterization of a rat model of diabetic nephropathy. Diabetes 53, 735–742.

Palygin, O., Evans, L.C., Cowley, A.W., Jr., and Staruschenko, A. (2017). Acute in vivo analysis of ATP release in rat kidneys in response to changes of renal perfusion pressure. J. Am. Heart Assoc. 6, e006658.

Palygin, O., Ilatovskaya, D.V., Levchenko, V., Klemens, C.A., Dissanayake, L., Williams, A.M., Pavlov, T.S., and Staruschenko, A. (2018). Characterization of purinergic receptor expression in ARPKD cystic epithelia. Purinergic Signal. 14, 485–497.

Palygin, O., Levchenko, V., Ilatovskaya, D.V., Pavlov, T.S., Ryan, R.P., Cowley, A.W., Jr., and Staruschenko, A. (2013). Real-time electrochemical detection of ATP and H(2)O(2) release in freshly isolated kidneys. Am. J. Physiol. Ren. Physiol. 305, F134–F141.

Palygin, O., Spires, D., Levchenko, V., Bohovyk, R., Fedoriuk, M., Klemens, C.A., Sykes, O., Bukowy, J.D., Cowley, A.W., Jr., Lazar, J., et al. (2019). Progression of diabetic kidney disease in

T2DN rats. Am. J. Physiol. Ren. Physiol. *317*, F1450–F1461.

Pereira, J.M.S., Barreira, A.L., Gomes, C.R., Ornellas, F.M., Ornellas, D.S., Miranda, L.C., Cardoso, L.R., Coutinho-Silva, R., Schanaider, A., Morales, M.M., et al. (2020). Brilliant blue G, a P2X7 receptor antagonist, attenuates early phase of renal inflammation, interstitial fibrosis and is associated with renal cell proliferation in ureteral obstruction in rats. BMC Nephrol. *21*, 206.

Perez-Flores, G., Levesque, S.A., Pacheco, J., Vaca, L., Lacroix, S., Perez-Cornejo, P., and Arreola, J. (2015). The P2X7/P2X4 interaction shapes the purinergic response in murine macrophages. Biochem. Biophys. Res. Commun. *467*, 484–490.

Potthoff, S.A., Stegbauer, J., Becker, J., Wagenhaeuser, P.J., Duvnjak, B., Rump, L.C., and Vonend, O. (2013). P2Y2 receptor deficiency aggravates chronic kidney disease progression. Front. Physiol. *4*, 234.

Rizzuto, R., Pinton, P., Ferrari, D., Chami, M., Szabadkai, G., Magalhaes, P.J., Di Virgilio, F., and Pozzan, T. (2003). Calcium and apoptosis: facts and hypotheses. Oncogene *22*, 8619–8627.

Roshanravan, H., and Dryer, S.E. (2014). ATP acting through P2Y receptors causes activation of podocyte TRPC6 channels: role of podocin and reactive oxygen species. Am. J. Physiol. Ren. Physiol. *306*, F1088–F1097.

Schneider, M., Prudic, K., Pippel, A., Klapperstuck, M., Braam, U., Muller, C.E., Schmalzing, G., and Markwardt, F. (2017). Interaction of purinergic P2X4 and P2X7 receptor subunits. Front. Pharmacol. *8*, 860.

Schwiebert, E.M., and Zsembery, A. (2003). Extracellular ATP as a signaling molecule for epithelial cells. Biochim. Biophys. Acta *1615*, 7–32.

Slaughter, T.N., Paige, A., Spires, D., Kojima, N., Kyle, P.B., Garrett, M.R., Roman, R.J., and Williams, J.M. (2013). Characterization of the development of renal injury in Type-1 diabetic Dahl salt-sensitive rats. Am. J. Physiol. Regul. Integr. Comp. Physiol. *305*, R727–R734.

Solini, A., Menini, S., Rossi, C., Ricci, C., Santini, E., Blasetti Fantauzzi, C., Iacobini, C., and Pugliese, G. (2013). The purinergic 2X7 receptor participates in renal inflammation and injury induced by high-fat diet: possible role of NLRP3 inflammasome activation. J. Pathol. *231*, 342–353.

Spires, D., Ilatovskaya, D.V., Levchenko, V., North, P.E., Geurts, A.M., Palygin, O., and Staruschenko, A. (2018). Protective role of Trpc6 knockout in the progression of diabetic kidney disease. Am. J. Physiol. Ren. Physiol. *315*, F1091–F1097.

Stockand, J.D., Mironova, E., Bugaj, V., Rieg, T., Insel, P.A., Vallon, V., Peti-Peterdi, J., and Pochynyuk, O. (2010). Purinergic inhibition of ENaC produces aldosterone escape. J. Am. Soc. Nephrol. *21*, 1903–1911.

Taylor, S.R., Turner, C.M., Elliott, J.I., McDaid, J., Hewitt, R., Smith, J., Pickering, M.C., Whitehouse, D.L., Cook, H.T., Burnstock, G., et al. (2009a). P2X7 deficiency attenuates renal injury in experimental glomerulonephritis. J. Am. Soc. Nephrol. *20*, 1275–1281.

Taylor, S.R., Turner, C.M., Elliott, J.I., McDaid, J., Hewitt, R., Smith, J., Pickering, M.C., Whitehouse, D.L., Cook, H.T., Burnstock, G., et al. (2009b). P2X7 deficiency attenuates renal injury in

experimental glomerulonephritis. J. Am. Soc. Nephrol. *20*, 1275–1281.

Umanath, K., and Lewis, J.B. (2018). Update on diabetic nephropathy: core curriculum 2018. Am. J. Kidney Dis. *71*, 884–895.

Vallon, V., and Komers, R. (2011). Pathophysiology of the diabetic kidney. Compr. Physiol. *1*, 1175–1232.

Vallon, V., Unwin, R., Inscho, E.W., Leipziger, J., and Kishore, B.K. (2020). Extracellular nucleotides and P2 receptors in renal function. Physiol. Rev. *100*, 211–269.

Vonend, O., Turner, C.M., Chan, C.M., Loesch, A., Dell'Anna, G.C., Srai, K.S., Burnstock, G., and Unwin, R.J. (2004a). Glomerular expression of the ATP-sensitive P2X receptor in diabetic and hypertensive rat models. Kidney Int. *66*, 157–166.

Vonend, O., Turner, C.M., Chan, C.M., Loesch, A., Dell'Anna, G.C., Srai, K.S., Burnstock, G., and Unwin, R.J. (2004b). Glomerular expression of the ATP-sensitive P2X receptor in diabetic and hypertensive rat models. Kidney Int. *66*, 157–166.

Wilson, P.C., Wu, H., Kirita, Y., Uchimura, K., Ledru, N., Rennke, H.G., Welling, P.A., Waikar, S.S., and Humphreys, B.D. (2019). The single-cell transcriptomic landscape of early human diabetic nephropathy. Proc. Natl. Acad. Sci. U S A *116*, 19619–19625.

Xia, J.F., Liang, Q.L., Hu, P., Wang, Y.M., Li, P., and Luo, G.A. (2009). Correlations of six related purine metabolites and diabetic nephropathy in Chinese type 2 diabetic patients. Clin. Biochem. *42*, 215–220.

STAR★METHODS

KEY RESOURCES TABLE

REAGENT OR RESOURCE	SOURCE	IDENTIFIER
Antibodies		
P2Y1	Alomone	Cat# APR-021; RRID:AB_10919250
P2Y2	Alomone	Cat# APR-010; RRID:AB_2040078
P2Y12	Alomone	Cat# APR-012; RRID:AB_2040074
P2X4	Alomone	Cat# APR-002; RRID:AB_2040058
P2X7	Alomone	Cat# APR-004; RRID:AB_2040068
P2X7 ext	Alomone	Cat# APR-008; RRID:AB_2040065
Gapdh	SantaCruz	Cat# sc-47724; RRID:AB_627678
Nephrin	SantaCruz	Cat# sc-377246
Donkey anti-mouse Alexa-488	Invitrogen	Cat# A21202; RRID:AB_141607
Donkey anti-rabbit Alexa-594	Invitrogen	Cat# A21207; RRID:AB_141637
Chemicals, peptides, and recombinant proteins		
RPMI1640	Invitrogen	Cat# 11835-030
BSA	Sigma	Cat# A3059
Fluoromount-G	ThermoFisher	Cat# 00-4958-02
TRIzol	ThermoFisher	Cat# 15596026
ATP	Sigma	Cat# A6559
Insulin pellets	LinShin Canada Inc.	Cat# LHR-10BV
Streptozotocin (STZ)	Sigma	Cat# S0130
MRS2500	Tocris	Cat# 2159
5-BDBD	Tocris	Cat# 3579
A 438079	Tocris	Cat# 2972
DMSO	Sigma	Cat# 276855
Critical commercial assays/kits		
Creatinine Assay	Cayman Chemical	Cat# 500701
Albumin Assay	Active Motif	Cat# 15002
RevertAid First Strand cDNA Synthesis Kit	ThermoSci	Cat# K1621
qPCR primers		
P2X4 Forward GACGTGGCGGACTATGTGAT Reverse TCTTCCAGTCGCAACTCCAC	This paper	N/A
P2X7 Forward CAAAGGTCAAGAGGTCCCGAGAC Reverse GCCCTGCGGTTCTCTGGTAG	This paper	N/A
P2Y1 Forward GGCCGACTTTTTGTATGTGCTC Reverse TCCCCGAAGATCCAGTCAGTC	This paper	N/A
P2Y2 Forward TCGTGGCCCTCTACATCTTCC Reverse CACCCTGGGCGTAGTAATAAACC	This paper	N/A
Gapdh Forward GGCAAATTCAACGGCACAGT Reverse AGATGGTGATGGGCTTCC C	This paper	N/A

Continued

REAGENT OR RESOURCE	SOURCE	IDENTIFIER
Fluorescent Dyes		
Hoescht	Sigma	Cat# H6024
Fluo4	Invitrogen	Cat# F23917
FuraRed	Invitrogen	Cat# F3021
Fura 2-TH	Setareh Biotech	Cat# 51419
Experimental models: Organisms/strains		
Rat: T2DN	MCW breeding colony	(Nobrega et al., 2004; Palygin et al., 2019)
Rat: Goto-Kakizaki, GK	MCW breeding colony	(Goto et al., 1976)
Rat: Wistar	Charles River Laboratories	https://www.criver.com/products-services/find-model/wistar-igs-rat?region=3611
Rat: Dahl salt-sensitive (SS or SS/JrHsdMcwi)	MCW breeding colony	(Palygin et al., 2019)
Software and algorithms		
Fiji (ImageJ 1.47v)	National Institute of Health, USA	https://imagej.nih.gov/ij/
SigmaPlot 12.5	Systat Software, Inc	https://systatsoftware.com/
OriginPro 9.0	OriginLab Corporation	https://www.originlab.com/
Other		
0.4% NaCl AIN-76 diet	Dyets	Cat# D113755
Purina diet	LabDiet	Cat# 5001
Mesh sieve 73.7 μm	Sigma	Cat# S4145
Mesh sieve 150 μm	Fisher Sci	Cat# 04-881-5Z
Mesh sieve 106 μm	Fisher Sci	Cat# 04-881-5X
Glucometer strips	Bayer	Cat# 56-7080BX
Glass Bottom Cell Culture Dishes	Mattek	Cat# P35G-1.5-14-C

RESOURCE AVAILABILITY

Lead contact

Further information and requests for resources and reagents should be directed to and will be fulfilled by the lead contact, Alexander Staruschenko (staruschenko@mcw.edu).

Materials availability

This study did not generate new unique reagents.

Data and code availability

The datasets generated and/or analyzed during the current study are available from the corresponding author on reasonable request.

EXPERIMENTAL MODEL AND SUBJECT DETAILS

Animals

The animal use and welfare procedures adhered to the National Institutes of Health (NIH) Guide for the Care and Use of Laboratory Animals following protocols reviewed and approved by the Medical College of Wisconsin (MCW) Institutional Animal Care and Use Committee. To assess renal purinergic P2 signaling in T2D, male Wistar (nondiabetic), Goto-Kakizaki (GK; T2D), and T2DN rats at different ages (12 and >48 weeks old) were used. Wistar male rats were purchased from Charles River Laboratories. GK and T2DN rats have been inbred for multiple generations at MCW. Animals were fed a regular diet (#5001, Lab-Diet, Purina) with water and food provided ad libitum. Streptozotocin (STZ)-injected Dahl salt-sensitive (SS) rats (SS/JrHsdMcwi) were used to characterize P2-dependent calcium dynamics in podocytes in the conditions of T1D. Briefly, 65 mg/kg of streptozotocin was dissolved in citrate buffer and immediately administered via intraperitoneal injection (Ilatovskaya et al., 2015; Miller et al., 2018; Slaughter et al., 2013; Spires

et al., 2018). SS rats were also inbred for multiple generations at MCW and maintained on a 0.4% NaCl AIN-76 diet (#D113755, Dyets) in a standard 12/12 dark/light cycle. 8- to 9-week old SS rats were injected with STZ to induce T1D. Four days after injection, blood glucose levels were tested to verify successful beta-cell ablation as determined by blood glucose levels $\geq 300 mg/dL$, then implanted with a long-acting subcutaneous insulin pellet between scapulae (LinShin, Canada) to maintain moderate hyperglycemia as described (Ilatovskaya et al., 2015). Blood glucose levels, as determined by tail prick blood samples measured by a glucometer, were checked periodically (2, 6, 12, and 14 weeks). At the end of the experiment, urine samples collected for 24 hours in metabolic cages were used to determine volume, microalbumin and creatinine levels. Urinary microalbumin concentrations were determined by an albumin blue fluorescent assay kit (Active Motif) and read by a fluorescent plate reader (FL600, Bio-Tek). Urinary creatinine levels were determined by assay kit from Cayman Chemical. Albumin to Creatinine ratios (ACR) were determined by dividing microalbumin concentrations (mg/ml) by creatinine concentrations (mg/ml).

METHOD DETAILS

Glomeruli isolation

Freshly isolated kidney cortex was minced and sequentially pushed through a steel 150 μm mesh sieve and then pipetted through a 106 μm mesh sieve (#04-881-5Z and #04-881-5X; Fisher Sci) using the culture medium solution RPMI1640 (Invitrogen) with 5% BSA (RPMI-BSA solution). This tissue homogenate was then pipetted onto a 73.7 μm mesh sieve (#S4145; Sigma), leaving the glomeruli on the top surface. The glomeruli were rinsed using the RPMI-BSA solution into a 15 ml conical tube and pelleted for 10-15 min on ice. After sedimentation, the excess RPMI-BSA solution was removed, and the isolated decapsulated glomeruli were used for confocal microscopy experiments as described below.

Confocal calcium imaging in the podocytes of freshly isolated glomeruli

Glomeruli were imaged using confocal microscopy immediately after isolation. Glomerular fractions were loaded with Fura Red and Fluo-4 AM (2.5 μM of each, #F3021 and #F23917, correspondingly, Invitrogen) dyes for ~ 40 min at room temperature, then transferred to poly-L-lysine coated coverslips, allowed to attach to the glass surface for 5-10 min, and, then washed twice with a solution containing (in mM): 145 NaCl, 4.5 KCl, 2 CaCl$_2$, 2 MgCl$_2$, 10 HEPES, pH 7.35. Calcium imaging was performed on a Leica TCS SP5 63x/1.4 oil objective (x,y,t; 2.46 sec per frame) controlled by Leica Application Suite X software. For initial experiments measuring basal [Ca^{2+}]$_i$ and ATP response in 12 week old T2DN rats, fluorescence measurements were obtained on the confocal laser scanning microscope system Nikon A1-R (oil immersed Plan Apo 60x/NA 1.4 Oil objective) with the argon laser synchronous excitation at 488 nm and selective transmission of light through the emission filters 520/25 and 680/25 for Fluo-4 and Fura Red, respectively. Ratiometric fluorescence images of Fluo-4 (excitation at 488 nm and emission at 520 $\pm$ 20 nm) and Fura Red (excitation at 488 nm and emission at >600 nm) were obtained with the same instrument settings for all experiments in times series (xyt, 4 seconds per frame (Ilatovskaya et al., 2018). In some experiments, Fura Red was replaced with Fura 2-TH (ex. 488 em. >600 nm; #51419, Setareh Biotech, OR). Fluorescence images were collected with 0.25 Hz frequency and processed with open-source software Fiji (ImageJ 1.47v, National Institute of Health, USA). [Ca^{2+}]$_i$ concentration in podocytes preloaded with Fluo-4 and Fura Red was measured by application of 10 μM ionomycin followed by addition of 1 mM MnCl$_2$ to the bath solution. The bath solution contained (in mM) 145 NaCl, 4.5 KCl, 2 MgCl$_2$, 2 CaCl$_2$ and 10 HEPES (pH 7.35) (Palygin et al., 2018). The ratiometric fluorescence intensity values (Fluo4/FuraRed) were calculated by selecting podocytes as regions of interest in Fiji and baseline correction was performed in OriginPro 9.0 (MicroCal, Northhampton, MA). Individual Ca^{2+} transients evoked by the extracellular application of ATP in the presence or absence of corresponding P2 receptors inhibitors were baselined and summarized for all podocytes (at least 6 glomeruli per group from $\geq$ 4 animals). There was no significant difference between water or DMSO vehicle treated control glomeruli. We evaluated the changes in Ca^{2+} transient maximum amplitude or [Ca^{2+}]$_i$ (area under the curve) within the time interval from the start of the application until 400 s. To determine the relative contribution of different components of purinergic signaling (metabotropic and ionotropic) to the ATP response, we calculated the % of [Ca^{2+}]$_i$ response from control (bulk ATP response, no inhibitors) from [Ca^{2+}]$_i$ flux values in the presence of a specific antagonist or combination of inhibitors.

Western blotting

For preparation of kidney lysates, cortical sections were collected at the same time as glomerular isolation, snap frozen in liquid nitrogen, then weighed and dissolved in Laemmli with protease and phosphatase

inhibitors (Roche) at 20 mg/ml with pulse sonication for 15-20 sec. Samples were subjected to SDS-PAGE, transferred onto nitrocellulose membrane (Millipore) for antibody hybridization, and subsequently visualized by enhanced chemiluminescence (ECL; Amersham Biosciences). See Key Resources table for antibodies used for Western blot analysis.

mRNA isolation and PCR analysis

Total RNA from flash frozen cortical kidney sections was isolated using TRIzol Reagent (ThermoFisher) according to manufacturer's protocol. Total RNA quantity was determined by Nanodrop 2000 (ThermoFisher). RNA quality was verified using Agilent 2100 Bioanalyzer, and only samples with RNA integrity numbers (RIN) greater than 8 were used. cDNA from 2μg of RNA was generated using the RevertAid First Strand cDNA Synthesis Kit (ThermoFisher) with random hexamer primers. Real-time PCR reactions were carried out on an ABI Prism 7900HT (ABI, Applied Biosytems, Foster City, CA) using Bullseye EvaGreen qPCR Master Mix (MedSci, Valley Park, MO) according to manufacturer's directions with samples run in triplicate. Final Ct values were determined using SDS software, version 2.3. Exon spanning primers were designed from the rat sequences of *P2rx4*, *P2rx7*, *P2ry1*, *P2ry2* and *Gapdh* (see Key Resources Table). Quantification of *P2rx4*, *P2rx7*, *P2ry1* and *P2ry2* mRNA was determined by normalizing to *Gapdh*.

Immunofluorescence labeling

Freshly-isolated glomeruli were allowed to adhere to twice coated poly-l-lysine coverslips before washing with PBS and fixing with 4% paraformaldehyde in PBS for 20 minutes. Following 3x washes with PBS, glomeruli were blocked and permeabilized with 2% BSA + 0.25% Triton-X in PBS. Primary antibodies (1:100; Nephrin sc-377246, P2X$_4$ APR-002) were diluted in 2% BSA in PBS overnight at 4°C. The next day, glomeruli were washed 3x with PBS then incubated with Alexa-labeled secondary antibodies (1:500) for 1 hr at room temperature in 2% BSA in PBS. Following 3x washes with PBS, nuclei were labeled with 0.5 μg/mL Hoescht for 5 min, washed 5x with PBS and then mounted onto slides with Fluoromount-G. Images with 2 μm z-steps were captured on a Nikon A1R confocal inverted microscope using a Plan Apo ×40 DIC M N2 objective with 0.95 numerical aperture controlled by Nikon Elements AR software (Nikon, Tokyo, Japan). Post-image processing was performed with Fiji image software.

QUANTIFICATION AND STATISTICAL ANALYSIS

Data are presented as means $\pm$ SEM. In the box plot graphs, the box represents $\pm$ SE, and a line inside the box marks the median. The whiskers are $\pm$ SD. Data were tested for normality (Shapiro-Wilk) and equal variance (Levene's homogeneity test). Statistical analysis consisted of one-way ANOVA or student t-test as indicated (SigmaPlot 12.5 or OriginPro 9.0), with a p-value of <0.05 considered significant. Dunnett's or Tukey multiple-comparisons adjustment was applied to all pairwise p-values as indicated in the figure legends.